



## The Co<sup>2+</sup> and Ni<sup>2+</sup> complexes of 2-(2-(2-aminothiazol-4-yl)acetyl)-N-phenylhydrazine-1-carbothioamide ligand and evaluation of their biological potency

Huda Hamza<sup>a</sup>, Ahmed M. El-Demeri<sup>b</sup>, Gaber M. Abu El-Reash<sup>a,\*</sup>

<sup>a</sup> Chemistry Department, Faculty of Science, Mansoura University

<sup>b</sup> Oncology and Nuclear Medicine Department, Faculty of Medicine, Mansoura University

\* Correspondence to: gaelreash@mans.edu.eg, 01000373155)

Received: 12/11/2023  
Accepted: 9/1/2024

**Abstract:** The Co<sup>2+</sup> and Ni<sup>2+</sup> complexes of H<sub>2</sub>L ligand were isolated. By using a variety of methods, including elemental (CHN) analysis, FT-IR, UV-visible, and NMR spectroscopy, the assembly of the ligand and its chelates was completely clarified. Additionally, measurements of magnetic field strength and molar conductance were made. Thermal measurements using TG and DTG were made. Horowitz and Coats equations were used to discuss the complex's thermodynamic and kinetic properties. Finally, the compound under test had its biological activity assessed.

**keywords:** Complexes, TG measurements, kinetic studies, biological activity

### 1. Introduction

One of nature's most resilient interactions is the development of metal complexes [1, 2]. The biological effects of pharmaceuticals can be impacted by the interaction of metal ions with proteins. The relationship between a drug's complexation, distribution, and absorption in the body, as well as how complexation affects the timing of a drug's action, has gained new prominence in pharmacy and medicine [3]. Sulfur and nitrogen compounds, as well as their metal complexes, have potent antimicrobial [4, 5], antifungal [6, 7], antibacterial [8, 9], anticarcinogenic [5, 8, 9], and insulin mimetic activities. The suppression of DNA fusion caused by a change in the reductive alteration of tri-nucleotide to deoxyribonucleotide may be the cause of antitumor activity [11]. Attributable to their extensive spectrum of biological potentialities, new thiosemicarbazides stand out within the sulfur family of ligating structures [12–15]. Their great ability to chelate with metal ions, which fungi need for their metabolism, is the key factor contributing to their biological efficiency. Another explanation for the anticancer and antibacterial effects of thiosemicarbazide complexes is their capacity to permeate among semipermeable cell

membranes and their increased lipophilicity in comparison to the ligand [16–19].

### 2. Materials and methods

#### 2.1. Materials

The 2-(2-(2-aminothiazol-4-yl)acetohydrazide, phenyl isothiocyanate, and metal salts were all employed in the experiment. Nitric acid (HNO<sub>3</sub>) and silver nitrate (AgNO<sub>3</sub>) were also bought from Sigma Aldrich. Merck provided organic solvents including dimethyl sulphoxide and pure ethanol.

#### 2.2. Characterization

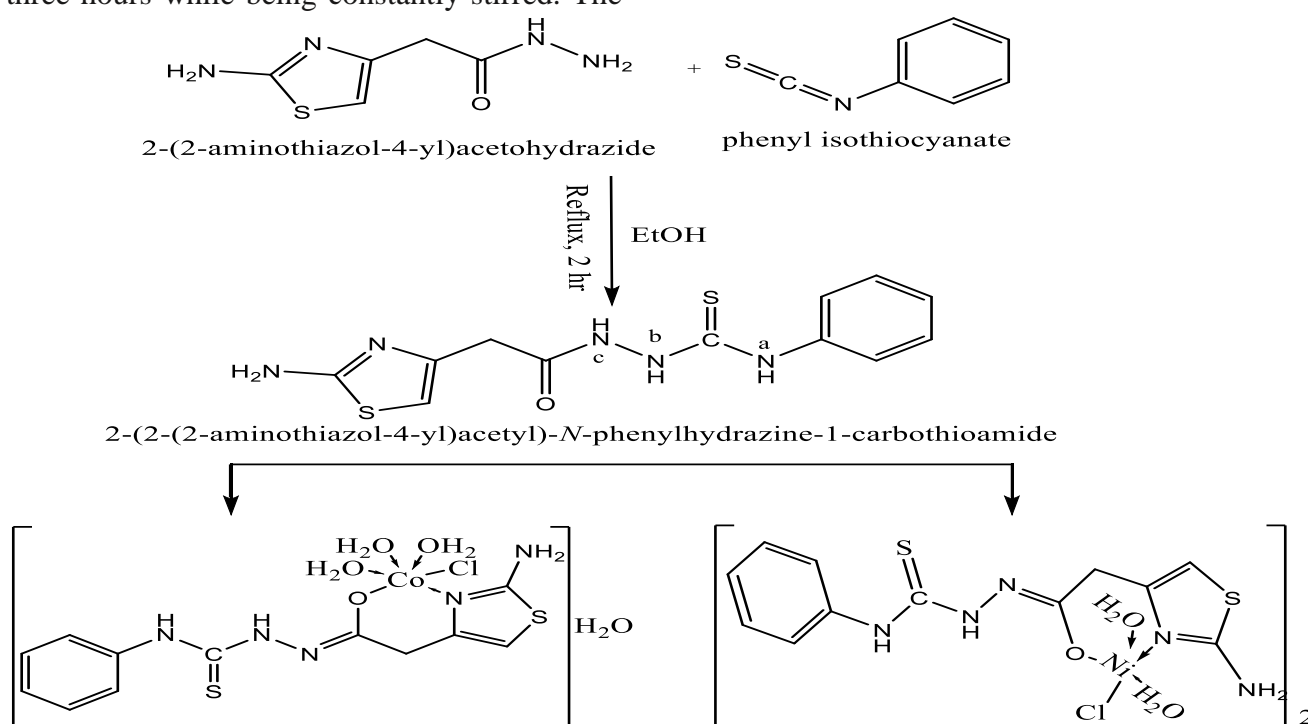
Perkin-Elmer 2400 analyzer was accustomed regulate the results of the elemental studies (C, H, and N). Volumetric and gravimetric studies were used to estimate the concentrations of Co<sup>2+</sup>, Ni<sup>2+</sup>, and Cl<sup>-</sup> ions [20]. The  $\mu_{\text{eff}}$  values of the paramagnetic complex was measured using the Sherwood magnetic susceptibility balance at room temperature. A Mattson 5000 FT-IR spectrophotometer was used for measuring FT-IR spectroscopy. Additionally, DMSO-based UV-Vis spectra were captured at room temperature on a UV2 Unicam spectrophotometer. For thermogravimetric analyses (TG, DTG) from 20 °-800 °C with heating rate (10 degree/min) and dynamic N<sub>2</sub> atmosphere (15 mL/min), a Shimadzu DTG50

thermogravimetric analyzer was employed. Finally, the synthesized complex's molar conductance of 110-3 M was measured using a DMSO solvent at room temperature using an AJENCO, vision plus EC 3175 conductivity meter.

### 2.3. Synthesis of ligand and its complexes

1.0 mmol of 2-(2-aminothiazol-4-yl)acetohydrazide and Phenyl isothiocyanate were mixed in an ethanolic solution, then the resulted mixture was warmed for two hours using reflux heating (scheme 1). Instantaneously, the solution took on a golden hue. The reaction mixture was then refluxed for three hours while being constantly stirred. The

reactions were refluxed with constant stirring for 5 hours for the Ni<sup>2+</sup> complex and 5 hours for the Co<sup>2+</sup> complex, respectively. For the Ni<sup>2+</sup> complex, a 5 ml solution of NiCl<sub>2</sub>.6H<sub>2</sub>O in ethanol (1.0 mmol) and a 5 ml solution of CoCl<sub>2</sub>.4H<sub>2</sub>O in ethanol (1.0 mmol) were added to two 20 ml ethanolic solutions of the ligand. After being completely cleaned with warm ethanol and maintained in a void desiccator concluded anhydrous calcium chloride, the isolated solid complex was filtered out. The separated complex had a high percentage yield (92%). Scheme 1 presents the researched complex's hypothesized structure.



Scheme 1: Synthesis of H<sub>2</sub>L and its complexes.

### 2.4. Biological studies

#### 2.4.1. Anti-microbial activities

The novel complexes under inquiry were examined using the described approach [21] for in vitro anti-microbial screening against several bacterial species. The % A.I. values were calculated via the subsequent equation:

$$\% \text{ A. I.} = \frac{\text{inhibition Zone by tested compound}}{\text{inhibition Zone by standard}} \times 100$$

#### 2.5. Cytotoxicity assay

- PC3 cells from humans. The property business for biotic products and vaccines (VACSERA), located in Cairo, Egypt, received the cell line
- from ATCC. As a benchmark anticancer medication, 5-fluorouracil was chosen.

- Chemical reagents: Fetal bovine serum (GIBCO, UK) besides the following: MTT, RPMI-1640 medium, 5-fluorouracil, and DMSO (Sigma Co., St. Louis, USA).
- **MTT assay [22]:** This assay was performed to assess the repressing properties of substances on cell growth using the cell line. This colorimetric assay depends on the alteration of the yellow tetrazolium bromide into a purple formazan derivative by living cells' mitochondrial succinate dehydrogenase. In RPMI-1640 medium of 10% fetal bovine fluid, PC3 was cultivated. At 37 degrees Celsius in an incubator with 5% CO<sub>2</sub>, antibiotics of 100 units.ml<sup>-1</sup> penicillin and 100 g.ml<sup>-1</sup> streptomycin were

introduced. A 96-well bowl with  $1.0 \times 10^4$  cells per well was used to seed the cell line [23] for 48 hours with 5%  $\text{CO}_2$  at 37 C. Subsequent incubation, the cells were uncovered to various chemical meditations and hatched for 24 hours. Following a 24-hour drug treatment period, 20 l of a 5-mg/ml MTT solution was applied and incubated for 4 hours. Each well receives 100 l of (DMSO) to melt the produced

formazan. Via EXL 800 a plate reader, the colorimetric test is measured and noted at an absorbance of 570 nm. Considered as  $(A_{570} \text{ of treated models} / A_{570} \text{ of untreated model}) \times 100$ , the relative cell viability was stated as a percentage.

### 3. Results and Discussion

The physical and analytical data of the isolated compounds are documented in **Table (1)**.

**Table (1):** The physical and analytical data of the ligand and its complexes.

Compound	M.wt.; ( $\text{g mol}^{-1}$ )	Color	M.P.; ( $^{\circ}\text{C}$ )	% Found (% Calc)					
				C	H	N	M	Cl	S
$\text{H}_2\text{L}$ ligand	307.39	Yellow	>300	46.45 (46.89)	4.15 (4.26)	22.32 (22.78)	-	-	21.13 (20.86)
$[\text{Co}(\text{HL})\text{Cl}(\text{H}_2\text{O})_3] \cdot \text{H}_2\text{O}$	472.83	Brownish orange	>300	30.23 (30.48)	4.92 (4.26)	14.23 (14.81)	12.15 (12.46)	8.00 (7.50)	13.10 (13.56)
$[\text{Ni}_2(\text{HL})_2\text{Cl}_2(\text{H}_2\text{O})_4]$	873.11	Brown	>300	33.52 (33.02)	3.92 (3.69)	16.23 (16.04)	13.68 (13.44)	7.85 (8.12)	14.95 (14.69)

#### 3.1. Molar conductance measurements

An important method for determining the precise structure of complexes, the amount of coordination, and the type of counter ions present inside or outside the coordination sphere in the synthesized complex is molar conductance analysis. As a result, it supports the complex's electrolytic nature [24]. At room temperature, in DMSO ( $1 \times 10^{-3}$  M), the molar conductance of  $[\text{Co}(\text{HL})\text{Cl}(\text{H}_2\text{O})_3]\text{H}_2\text{O}$  and  $[\text{Ni}_2(\text{HL})_2\text{Cl}_2(\text{H}_2\text{O})_4]$  complexes were measured. The non-electrolytic nature of both complexes is shown by their low conductance values, which are  $5\text{--}6 \text{ Ohm}^{-1}\text{cm}^2\text{mol}^{-1}$  [25].

#### 3.2. FT-IR spectroscopy

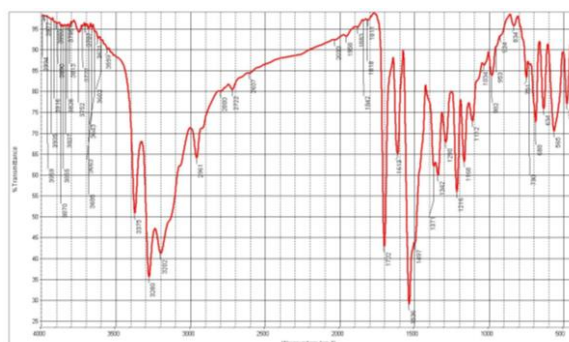
The IR spectrum of the ligand and it chelates as shown in **Fig. (1)** which demonstrates the vibration bands of the C=O, C=N, and C=S of the ligand at 1702, 1613, and 751  $\text{cm}^{-1}$  respectively. For  $\text{Co}^{2+}$  and  $\text{Ni}^{2+}$  complexes, the C=O vibrational band disappeared with appearance of a new band at 1623-1624  $\text{cm}^{-1}$  for  $\text{Ni}^{2+}$  and  $\text{Co}^{2+}$  complexes, respectively, characteristic for the new C=N group formed upon chelation. Additionally, the C=S

vibrational band appeared at 754  $\text{cm}^{-1}$  indicating that it is out of chelation in both complexes. Also, the C=N band shifted to 1565-1544  $\text{cm}^{-1}$ , for  $\text{Ni}^{2+}$  and  $\text{Co}^{2+}$  complexes, respectively. Two bands are detected in the

areas 549 and 453  $\text{cm}^{-1}$  attributable to M-O and M-N vibration bands, independently. ligand acts as (ON) mono-negative bidentate ligand around the  $\text{Co}^{2+}$  and  $\text{Ni}^{2+}$  centers.

#### 3.3. UV-visible and magnetic moment studies

The UV-vis absorptions of the ligand **Fig. (2)** display absorptions at  $\lambda(\text{nm})$ : 274 ( $\pi^* \leftarrow \pi$  in ph-ring), 358 ( $\pi^* \leftarrow \pi$  in C = S), 395 ( $\pi^* \leftarrow \pi$  in CO), and 445 ( $\pi^* \leftarrow n$  in CN) [26, 27]. The electronic spectral bands of  $[\text{Ni}_2(\text{HL})_2\text{Cl}_2(\text{H}_2\text{O})_4]$  as appeared in **Fig. (2)** at 425 and 390 nm may be due to  ${}^3\text{A}_{2g} \rightarrow {}^3\text{T}_{1g}(\text{P})$  and  ${}^3\text{A}_{2g} \rightarrow {}^3\text{T}_{1g}(\text{F})$  transitions, discretely. Also, value of the magnetic moment equals (2.87 B.M) which proves its octahedral stereochemistry around  $\text{Ni}^{2+}$  ion. While in electronic spectrum of  $\text{Co}^{2+}$  complex, two bands at 514 nm, besides 568 nm allocated to  ${}^4\text{T}_{1g}(\text{F}) \rightarrow {}^4\text{T}_{1g}(\text{P}) \nu_3$ , in addition  ${}^4\text{T}_{1g}(\text{F}) \rightarrow {}^4\text{A}_{2g}(\text{F}) \nu^2$  shifts in octahedral geometry [28].



**A**

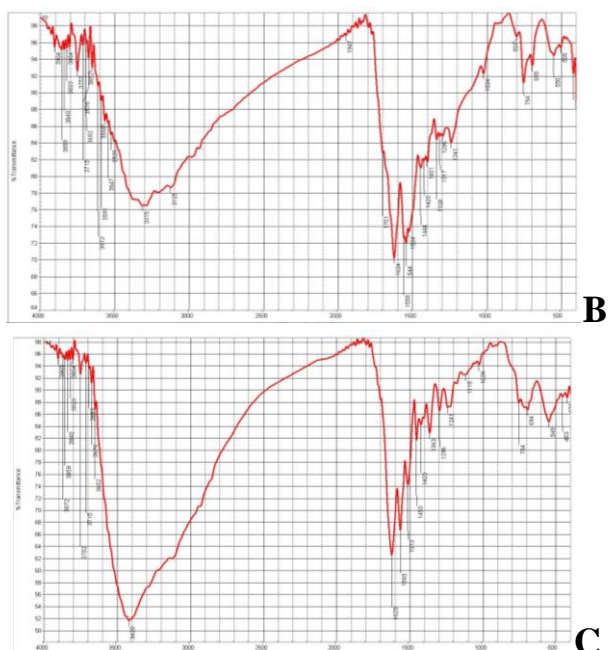


**Fig. (1):** IR spectrum of A: H<sub>2</sub>L ligand, B: Co<sup>2+</sup> complex, C: Ni<sup>2+</sup> complexes

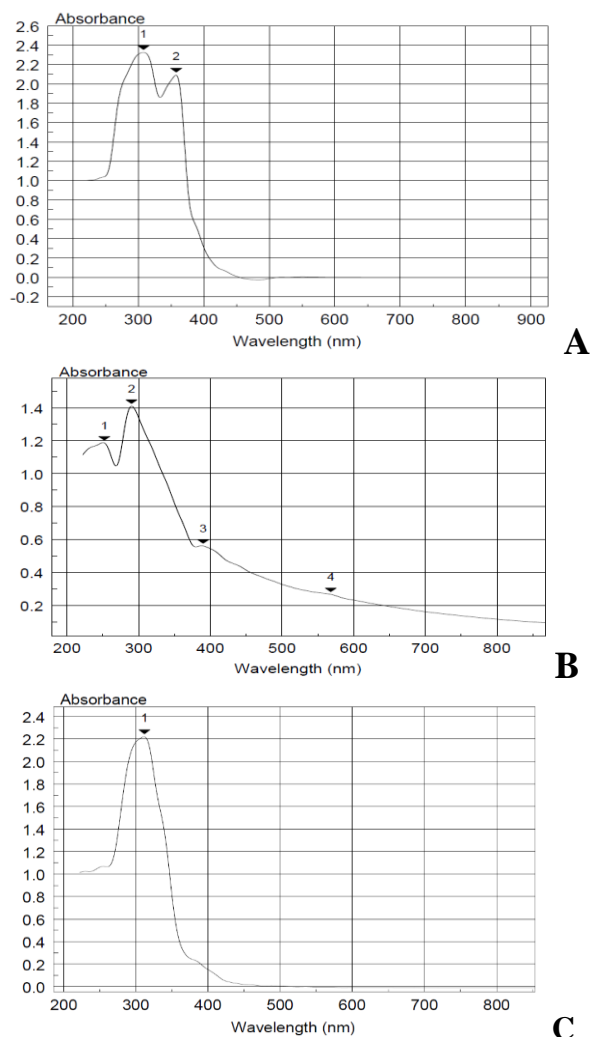


**Fig. (2):** Electronic absorption spectrum of AH<sub>2</sub>L ligand, B: Co<sup>2+</sup> complex, C: Ni<sup>2+</sup> complexes.

### 3.4. Thermal studies

The TG curve of [Co(HL)Cl(H<sub>2</sub>O)<sub>3</sub>].H<sub>2</sub>O **Fig. (3)** demonstrated five steps of thermal

decomposition. As discussed in **Table (2)**, The 1<sup>st</sup> step in 37 - 191°C range by a loss matching to 2H<sub>2</sub>O molecules (Found: 7.47 %; Calc: 7.62 %). The 2<sup>nd</sup> step lay in 191- 268 °C and assigned to the loss of 2H<sub>2</sub>O (coordinated water) fragment (Found: 7.74 %; Calc: 7.62 %). The 3<sup>rd</sup> step occurred in 268 – 502 °C and is because of losing HCl + C<sub>6</sub>H<sub>8</sub>N fragments (Found: 27.91 %; Calc: 27.62 %). The fourth step lied in the range 502 – 795 °C and assigned to the loss of C<sub>4</sub>H<sub>3</sub>N<sub>4</sub>S<sub>2</sub> fragment (Found: 36.00 %; Calcd.: 36.21 %) Finally, the residual part in the temperature range 795-800 °C referred to CoO + C<sub>2</sub> in which the calculated loss was in match with the found loss (Found: 21.13 %; Calcd.: 20.93 %).

### 3.5. Kinetic studies

Eyring equations [29, 30] were applied to calculate the thermodynamic and kinetic parameters. Data documented in **Table (3)** supposed that the decomposition stages are endothermic that was showed by the positive sign of ΔH<sup>\*</sup> value. Also, the degradation steps have a negative sign for entropies (ΔS<sup>\*</sup>) values indicating the well-ordered activated complex

than the reactants.

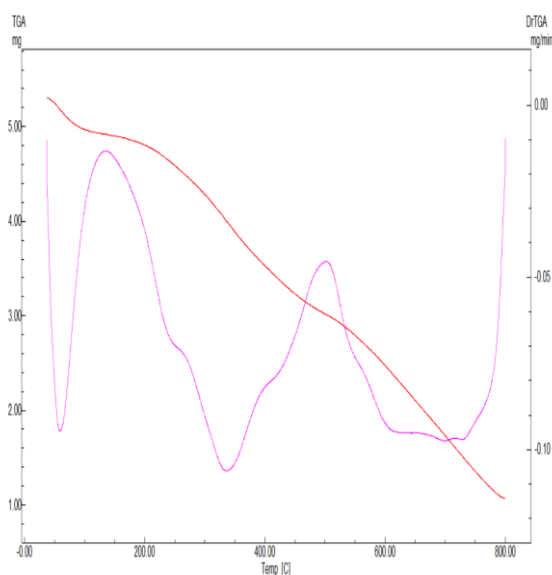


**Fig. (3):** TG and DTG curves of [Co(HL)Cl(H<sub>2</sub>O)<sub>3</sub>].H<sub>2</sub>O complex.

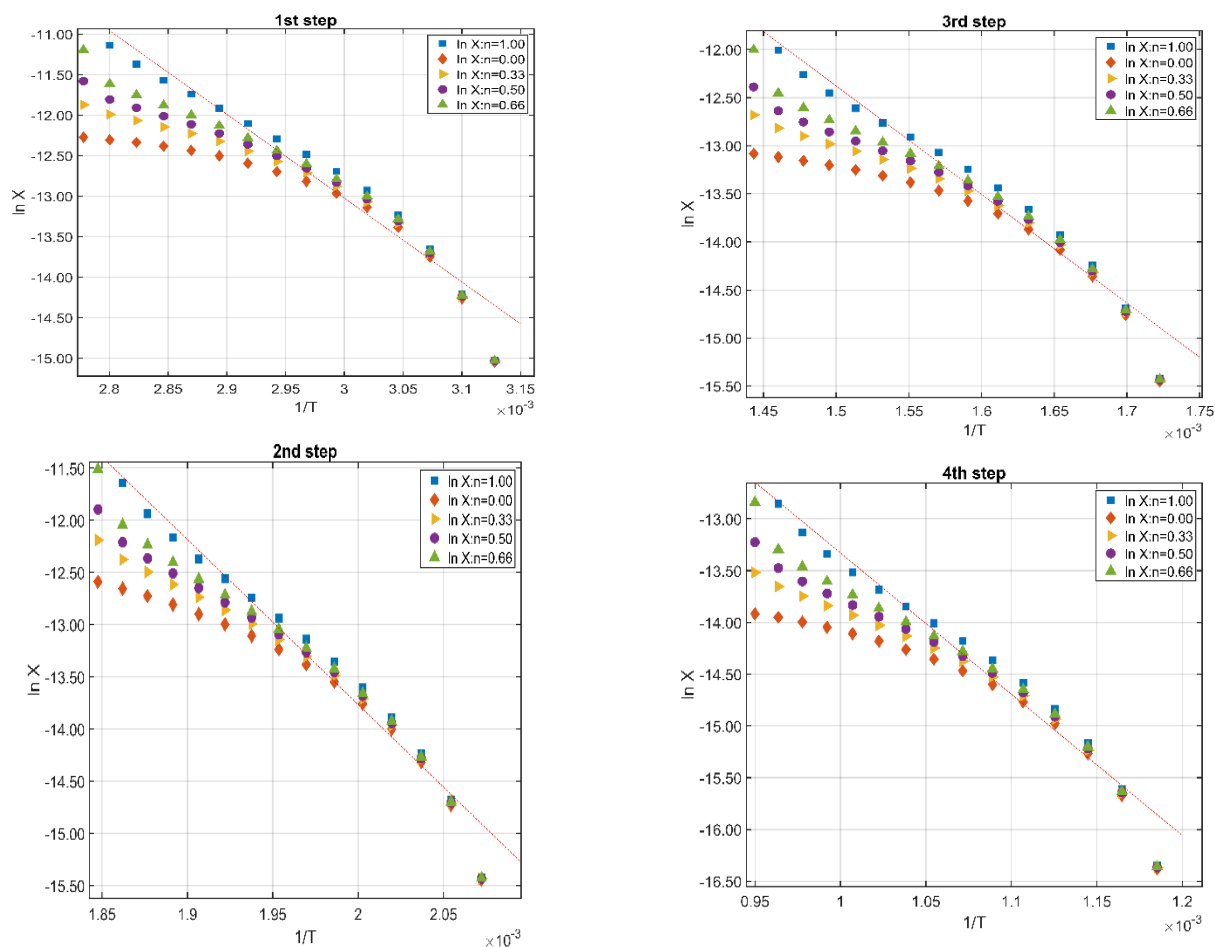
**Table (2):** Decompositions steps and removed species for  $[\text{Co}(\text{HL})\text{Cl}(\text{H}_2\text{O})_3]\cdot\text{H}_2\text{O}$  complex

.Compound	Temp. Range (°C)	Removed fragments	%Wt. Loss	
			Found	Calculated
$[\text{Co}(\text{HL})\text{Cl}(\text{H}_2\text{O})_3]\cdot\text{H}_2\text{O}$ $\text{C}_{12}\text{H}_{20}\text{ClCoN}_5\text{O}_5\text{S}_2$	37 - 191	$2\text{H}_2\text{O}$	7.47	7.62
	191- 268	$2\text{H}_2\text{O}$	7.74	7.62
	268 – 502	$\text{HCl} + \text{C}_6\text{H}_8\text{N}$	27.91	27.62
	502 - 795	$\text{C}_4\text{H}_3\text{N}_4\text{S}_2$	36.00	36.21
	795-800	Residue: $\text{CoO} + \text{C}_2$	21.13	20.93

Finally, positive values of  $(\Delta G^*)$  Gibbs free energy value clarify the non-spontaneous degradation stages. **Fig. (4)** and **Fig. (5)** display Horowitz-Metzger and Coats- Redfern schemes for  $[\text{Co}(\text{HL})\text{Cl}(\text{H}_2\text{O})_3]\cdot\text{H}_2\text{O}$  complex.

**Table (3):** Kinetic Parameters assessed via Horowitz and Coats methods for  $[\text{Co}(\text{HL})\text{Cl}(\text{H}_2\text{O})_3]\cdot\text{H}_2\text{O}$  complex.

Method	Peak	Mid Temp(K)	$E_a$ KJ/mol	A ( $\text{S}^{-1}$ )	$\Delta H^*$ KJ/mol	$\Delta S^*$ KJ/mol.K	$\Delta G^*$ KJ/mol
Coats-Redfern method	1 <sup>st</sup>	337.8	91.018	$1.14 \times 10^{12}$	88.209	-0.0151	93.304
	2 <sup>nd</sup>	500.66	134.783	$3.343 \times 10^{11}$	130.621	-0.0285	144.938
	3 <sup>rd</sup>	622.28	100.739	695951.64	95.5658	-0.13917	182.169
	4 <sup>th</sup>	928.36	125.751	16021.988	118.0326	-0.17385	279.428
Horowitz-Metzger method	1 <sup>st</sup>	337.8	86.041	$2.044 \times 10^{11}$	83.232	-0.0294	93.169
	2 <sup>nd</sup>	500.66	131.518	$1.627 \times 10^{11}$	127.355	-0.0346	144.669
	3 <sup>rd</sup>	622.28	93.8368	200442.81	88.6631	-0.1495	181.706
	4 <sup>th</sup>	928.36	113.439	3608.4684	105.7204	-0.1862	278.622

**Fig. (4):** Coats- Redfern plots for  $[\text{Co}(\text{HL})\text{Cl}(\text{H}_2\text{O})_3]\cdot\text{H}_2\text{O}$  complex

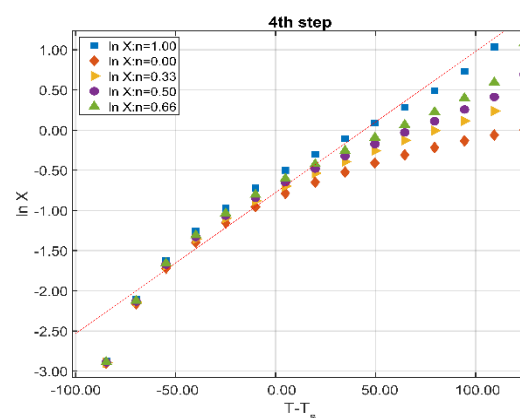
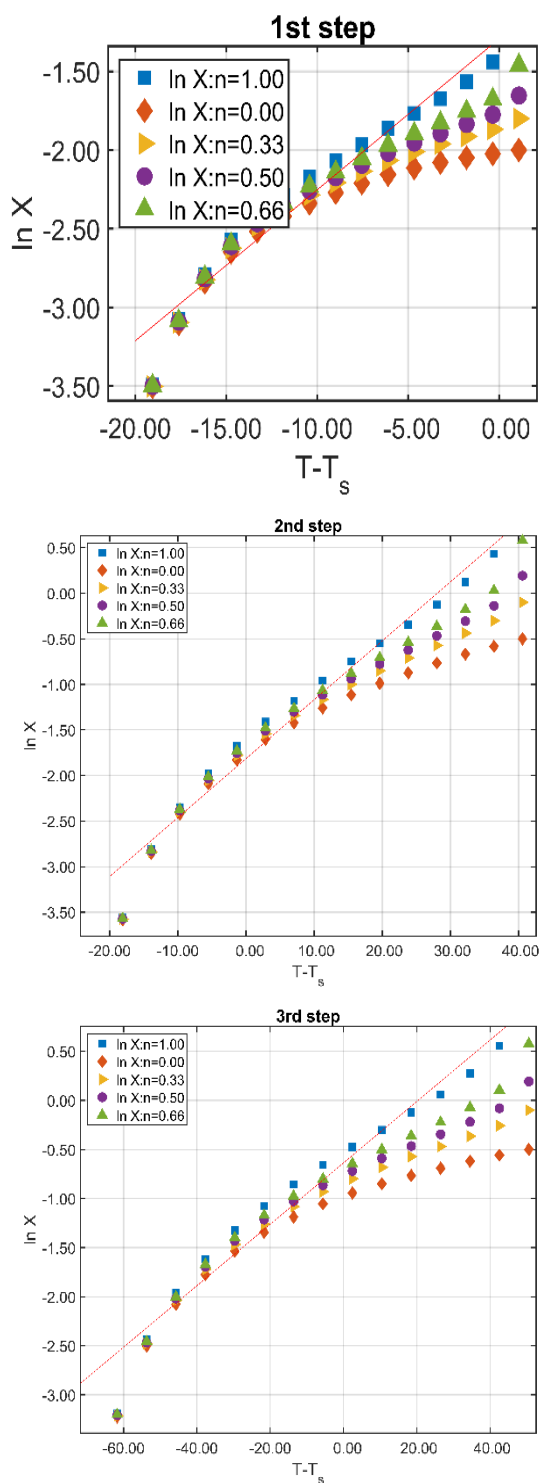


**Fig. (5):** Horowitz-Metzger plots for  $[\text{Co}(\text{HL})\text{Cl}(\text{H}_2\text{O})_3]\cdot\text{H}_2\text{O}$  complex

### 3.6. Biological potency

#### 3.6.1. Antimicrobial studies

The examined chemical complex underwent in vitro antimicrobial screening in contradiction of a panel of  $G^+$ : *s. aureus*,  $G^-$ : *e. coli* bacteria, and two different types of fungi, *Candida albicans* and *Saccharomyces cerevisiae*. As a typical check for antibacterial activity, ampicillin was utilized. Additionally, as shown in **Table (4)**, clotrimazole was utilized as a benchmark control in cases with antifungal activity.

#### 3.6.2. Cytotoxicity assay

The MTT assay is a colorimetric viability assay based on how the MTT molecule changes color in the presence of living cells. By measurement of absorbance, related to the number of feasible cells, and linking it to untreated panels, it is possible to assess the effectiveness of the tested medications to suppress cell growth. The MTT assay is a very helpful technique for figuring out how well novel cytotoxic mixtures work because of their rapidity, correctness, and capacity to examine a variety of cell sorts. **Table 5** displays the outcomes that were attained.

**Table (4):** Bacterial sensitivity (mm) of the isolated compounds against different bacterial and fungi strains.

Compound	S. aureus		E. coli		S. Cerevisiae		C. Albicans	
	inhibition zone	% A.I						
H <sub>2</sub> L	----	----	----	----	----	----	12	46
Co <sup>2+</sup> complex	31	140.9	----	----	----	----	----	----
Ni <sup>2+</sup> complex	----	----	28	116.7	38	135.7	22	84.6
Ampicillin	22	100	24	100	----	----	----	----
Colitrimazole	----	----	----	----	28	100	26	100

**Table 5:** In vitro Cytotoxicity outcomes for the isolated compounds.

Compounds	In vitro Cytotoxicity IC <sub>50</sub> (µg/ml)•
5-Fu	5.7±0.15
H <sub>2</sub> L	8.3±0.24
Co <sup>2+</sup> complex	65.1±4.30
Ni <sup>2+</sup> complex	17.0±1.21

**IC<sub>50</sub> (µg/ml):** above 100 (non-cytotoxic), 51 – 100 (weak), 21 – 50 (moderate), 11 – 20 (strong), and 1 – 10 (very strong).

**Table 6:** erythrocyte hemolysis outcomes for isolated compounds.

Compounds	Erythrocyte hemolysis A/B x 100	
	Absorbance of samples (A)	% hemolysis
Absorbance of H <sub>2</sub> O (B)	0.922	100%
Vit - C	0.026	2.8%
L1	0.030	3.2%
L1Ni	0.031	3.4%
L1Co	0.029	3.1%

### 3.6.3. Assay for erythrocyte hemolysis

Rats' hearts were punctured to obtain their blood, which was then collected in heparinized tubes. The buffy coat and plasma were removed, and erythrocytes were then splashed 3 times with 10 volumes of (0.15 M NaCl). The erythrocyte was spun at 2.50 rpm for 10 minutes during the final washing to create a continuously packed cell preparation. In this assay technique, peroxy radicals were the mediators of erythrocyte hemolysis [31]. In the same amount of 200 mM 2,2-azobis (2-amidinopropane) dihydrochloride (AAPH) solution (in PBS) containing materials to be evaluated at several concentrations, a 10% suspension of erythrocytes in pH 7.4 PBS (phosphate buffered saline) was added. The reaction mixture was gently shaken throughout its hour-long incubation at 37 °C. Following the removal of the reaction mixture, it was centrifuged at 2.500 rpm for 10 minutes after being diluted with 8 volumes of PBS. At 540 nm, the supernatant's absorbance A was measured. To ensure comprehensive hemolysis, the reaction mixture was similarly treated with

8 volumes of distilled water. The absorbance B of the supernatant produced after centrifugation was then measured at 540 nm. Equation (A/B) x 100% was used to compute the percentage of hemolysis. The information was displayed as mean and standard deviation. The positive control used was L-ascorbic acid. The results are displayed in table 6.

### 4. Conclusion

In the current work, its Co<sup>2+</sup> and Ni<sup>2+</sup> complexes as well as a novel thiosemicarbazide ligand were identified. The outcomes showed that Co<sup>2+</sup> and Ni<sup>2+</sup> ions are surrounded by octahedral geometry in the novel complexes. The ligand exhibited mononegative bidentate (ON) behavior around the metal core, according to infrared spectroscopy. The quantity of water molecules inside and outside the coordination sphere of the complex was revealed by thermal experiments. The Eyring equations were used in evaluation of the kinetic and thermodynamic parameters. Finally, the complex's biological activity was covered.

### 4. References

- 1 A. Sigel, H. Sigel, (2002). Metals ions in biological system: Volume 39: Molybdenum and tungsten: Their roles in biological processes, CRC press,
- 2 G.L. Eichhorn, (1973). Inorganic biochemistry, Elsevier Amsterdam,
- 3 M. Koutlemani, P. Mavros, A. Zouboulis, K. Matis, (1994) Sep. Sci. Technol., 29 867-886.
- 4 D.C. Quenelle, K.A. Keith, E.R. Kern, (2006) Antiviral Res., 71 24-30.
- 5 Y. Teitz, D. Ronen, A. Vansover, T. Stematsky, (1994) J. Riggs, Antiviral Res., 24 305-314.
- 6 M.C. Rodríguez-Argüelles, E.C. López-Silva, J. Sanmartín, P. Pelagatti, F. Zani, (2005) J. Inorg. Biochem., 99 2231-2239.
- 7 A. Cukurovali, I. Yilmaz, S. Gur, C. Kazaz, (2006) Eur. J. Med. Chem., 41 201-207.
- 8 A. Murugkar, B. Unnikrishnan, S. Padhye, R. Bhonde, S. Teat, E. Triantafillou, E. Sinn, (1999) Met.-Based Drugs, 6 177-182.
- 9 W. Hu, W. Zhou, C. Xia, X. Wen, (2006) Bioorg. Med. Chem. Lett., 16 2213-2218.

- 10 Z. Afrasiabi, E. Sinn, S. Padhye, S. Dutta, S. Padhye, C. Newton, C.E. Anson, A.K. Powell, (2003) *J. Inorg. Biochem.*, 95 306-314.
- 11 T. Bal-Demirci, M. Şahin, M. Özyürek, E. Kondakçı, B. Ülküseven, (2014) *Spectrochim. Acta, Part A*, 126 317-323.
- 12 D.X. West, A.E. Liberta, S.B. Padhye, R.C. Chikate, P.B. Sonawane, A.S. Kumbhar, R.G. Yerande, (1993) *Coord. Chem. Rev.*, 123 49-71.
- 13 M.B. Ferrari, G.G. Fava, E. Leporati, G. Pelosi, R. Rossi, P. Tarasconi, R. Albertini, A. Bonati, P. Lunghi, S. Pinelli, *J. Inorg. Biochem.*, 70 (1998) 145-154.
- 14 P. Sonawane, R. Chikate, A. Kumbhar, S. Padhye, R.J. Doedens, *Polyhedron*, 13 (1994) 395-401.
- 15 D.X. West, S.B. Padhye, P.B. Sonawane, *Complex Chemistry*, (1991) 1-50.
- 16 A.M. Thomas, A.D. Naik, M. Nethaji, A.R. Chakravarty, *Inorg. Chim. Acta*, 357 (2004) 2315-2323.
- 17 H. Beraldo, D. Gambinob, *Mini Rev. Med. Chem.*, 4 (2004) 31-39.
- 18 M.B. Ferrari, F. Bisceglie, G.G. Fava, G. Pelosi, P. Tarasconi, R. Albertini, S. Pinelli, (2002) *J. Inorg. Biochem.*, 89 36-44.
- 19 H. Seleem, B. El-Shetary, S. Khalil, M. Mostafa, M. Shebl, (2005) *J. Coord. Chem.*, 58 479-493.
- 20 A.I. Vogel, (1991). *Vogel's Textbook of quantitative chemical analysis*, 5th ed., John Wiley & Sons, New work
- 21 R.R. Zaky, T.A. Yousef, K.M. Ibrahim, (2012) *Spectrochim. Acta A* 97 683-694.
- 22 F. Denizot, R. Lang. (1986) *J. Immunol. Methods* 22 271-277.
- 23 H. J. Mauceri, N.N. Hanna, M. A. Beckett, D. H. Gorski, M. J. Staba, K. A. Stellato, K. Bigelow, R. Heimann, S. Gately, M. Dhanabal, G. A. Soff, V. P. Sukhatme, D. W. Kufe, R. R. (1998) *Weichselbaum. Nature*; 394:287-291
- 24 R.G. Deghadi, W.H. Mahmoud, G.G. Mohamed, *Appl. (2020) Organometal. Chem.* 34 (10) e5883.
- 25 J.W. Geary, (1971) The use of conductivity measurements in organic solvents for the characterization of coordination compounds, *Chem. Coord. Rev.* 7 (1) 81-122.
- 26 A.B.P. Lever, (1968). *Inorganic electronic spectroscopy, Studies in physical and theoretical chemistry Elsevier, Amsterdam* 33
- 27 T.A. Fayed, M. Gaber, G.M. Abu El-Reash, M.M. El-Gamil, (2020) *Appl. Organometal. Chem.* 34 (9) e5800.
- 28 M. Gaber, T.A. Fayed, M.M. El-Gamil, G.M. Abu El-Reash, (2018) *J. Mol. Str.* 1151 56-72.
- 29 A. Coats, J. Redfern, (1964) Kinetic parameters from thermogravimetric data, *Nature*, 201 (4914) 68-69.
- 30 H.H. Horowitz, G. Metzger, (1963) A new analysis of thermogravimetric traces, *Anal. Chem.* 35 (10) 1464-1468.
- 31 Y..Morimoto, K.Tanaka, Y. Iwakiri, S. Tokuhira, S. Fukushima, Y. Takeuchi, (1995) *Biol. Pharm.Bull.* 18 1417-1422.